Loss of c-Jun N-terminal Kinase 1 and 2 Function in Liver Epithelial Cells Triggers Biliary Hyperproliferation Resembling Cholangiocarcinoma

Francisco Javier Cubero,[1-3*] Mohamed Ramadan Mohamed,[1,4*] Marius M. Woitok,[1] Gang Zhao,[1] Maximilian Hatting,[1] Yulia A. Nevzorova,[1,5] Chaobo Chen,[2] Johannes Haybaeck,[6-8] Alain de Bruin,[9,10] Matias A. Avila,[11-13] Mark V. Boekschoten,[14] Roger J. Davis,[15] and Christian Trautwein[1]

Targeted inhibition of the c-Jun N-terminal kinases (JNKs) has shown therapeutic potential in intrahepatic cholangiocarcinoma (CCA)-related tumorigenesis. However, the cell-type-specific role and mechanisms triggered by JNK in liver parenchymal cells during CCA remain largely unknown. Here, we aimed to investigate the relevance of JNK1 and JNK2 function in hepatocytes in two different models of experimental carcinogenesis, the dethylnitrosamine (DEN) model and in nuclear factor kappa B essential modulator (NEMO)$^{\text{hepatocyte-specific knockout (}\Delta\text{hepa)}}$ mice, focusing on liver damage, cell death, compensatory proliferation, fibrogenesis, and tumor development. Moreover, regulation of essential genes was assessed by reverse transcription polymerase chain reaction, immunoblottings, and immunostainings. Additionally, specific *Jnk2* inhibition in hepatocytes of NEMO$^{\Delta\text{hepa}}$/JNK1$^{\Delta\text{hepa}}$ mice was performed using small interfering (si) RNA (si*Jnk2*) nanodelivery. Finally, active signaling pathways were blocked using specific inhibitors. Compound deletion of *Jnk1* and *Jnk2* in hepatocytes diminished hepatocellular carcinoma (HCC) in both the DEN model and in NEMO$^{\Delta\text{hepa}}$ mice but in contrast caused massive proliferation of the biliary ducts. Indeed, *Jnk1/2* deficiency in hepatocytes of NEMO$^{\Delta\text{hepa}}$ (NEMO$^{\Delta\text{hepa}}$/JNK$^{\Delta\text{hepa}}$) animals caused elevated fibrosis, increased apoptosis, increased compensatory proliferation, and elevated inflammatory cytokines expression but reduced HCC. Furthermore, si*Jnk2* treatment in NEMO$^{\Delta\text{hepa}}$/JNK1$^{\Delta\text{hepa}}$ mice recapitulated the phenotype of NEMO$^{\Delta\text{hepa}}$/JNK$^{\Delta\text{hepa}}$ mice. Next, we sought to investigate the impact of molecular pathways in response to compound JNK deficiency in NEMO$^{\Delta\text{hepa}}$ mice. We found that NEMO$^{\Delta\text{hepa}}$/JNK$^{\Delta\text{hepa}}$ livers exhibited overexpression of the interleukin-6/signal transducer and activator of transcription 3 pathway in addition to epidermal growth factor receptor (EGFR)-rapidly accelerated fibrosarcoma (Raf)-mitogen-activated protein kinase kinase (MEK)-extracellular signal-regulated kinase (ERK) cascade. The functional relevance was tested by administering lapatinib, which is a dual tyrosine kinase inhibitor of erythroblastic oncogene B-2 (ErbB2) and EGFR signaling, to NEMO$^{\Delta\text{hepa}}$/JNK$^{\Delta\text{hepa}}$ mice. Lapatinib effectively inhibited cystogenesis, improved transaminases, and effectively blocked EGFR-Raf-MEK-ERK signaling. *Conclusion*: We define a novel function of JNK1/2 in cholangiocyte hyperproliferation. This opens new therapeutic avenues devised to inhibit pathways of cholangiocarcinogenesis. (*Hepatology Communications* 2020;4:834-851).

Bile duct hyperplasia and aberrant cholangiocyte growth can result in hepatic cystogenesis, differentially diagnosed on the basis of cholangioma, cholangiofibrosis, intrahepatic cholangiocarcinoma (CCA), and oval cell hyperplasia.[1,2] CCA, a malignancy that arises in the setting of chronic inflammation of biliary epithelium cells, has an increasing incidence and is the second most common primary

Abbreviations: α-SMA, alpha smooth muscle actin; Δhepa, hepatocyte-specific knockout; A6, Notch-1; ALT, alanine aminotransferase; AST, aspartate aminotransferase; BW, body weight; CAF, cancer-associated fibroblast; CC3, cleaved caspase 3; CCA, cholangiocarcinoma; CK, creatine kinase; CLD, chronic liver disease; Col1A1, collagen type I alpha 1; DEN, diethylnitrosamine; dmbt1, deleted in malignant brain tumors 1; ECM, extracellular matrix; EGFR, epidermal growth factor receptor; EMT, epithelial–mesenchymal transition; ERBB, erythroblastic oncogene B; ERK, extracellular signal-regulated kinase; f/f, floxed mice; gabrp, gamma-aminobutyric acid A receptor, pi; GAPDH, glyceraldehyde 3-phosphate dehydrogenase; HCC, hepatocellular carcinoma; HER, human epidermal growth factor receptor; HNF, hepatocyte nuclear factor; HPF, high-power field; IHC, immunohistochemistry; IL, interleukin; JAK, Janus kinase; JNK, c-Jun N-terminal kinases; LoxP, locus of X-over P1; LPC, liver parenchymal cell; LW, liver weight; MAPK, mitogen-activated protein kinase; MEK, mitogen-activated protein kinase kinase; mRNA, messenger

liver cancer globally. Unfortunately, survival beyond a year of diagnosis is less than 5% and therapeutic options are scarce.[3]

Several *in vivo* and *in vitro* models as well as research with human tissue samples help to elucidate the main pathways implicated in CCA formation. However, none of these studies recapitulates the human disease, and translation into improved patient outcome has not been achieved. In addition, the pathophysiology of CCA remains poorly understood. Thus, there is an urgent need for new models to improve the management of this insidious and devastating disease.

RNA; MUC, mucin; NEMO, nuclear factor kappa B essential modulator; NF-κB, nuclear factor kappa B; OSM, oncostatin M; p, phosphorylated; PCNA, proliferating cell nuclear antigen; qRT-PCR, quantitative reverse-transcription polymerase chain reaction; Raf, rapidly accelerated fibrosarcoma; RIPK, receptor-interacting serine/threonine-protein kinase; si, small interfering; SOCS3, suppressor of cytokine signaling 3; SOX-9, transcription factor SOX 9; STAT, signal transducer and activator of transcription; TKI, tyrosine kinase inhibitor; TNF, tumor necrosis factor; TUNEL, terminal deoxynucleotidyl transferase–mediated deoxyuridine triphosphate nick-end labeling.

Received December 13, 2019; accepted February 7, 2020.

Additional Supporting Information may be found at onlinelibrary.wiley.com/doi/10.1002/hep4.1495/suppinfo.

**These authors contributed equally to this work.*

Supported by the Interdisciplinary Center for Clinical Research (IZKF), the SFB TRR 57, the CRC 1382, the DFG TR285-10/1, the German Krebshilfe (Grant 70113000), the RTG 2375 Tumor-Targeted Drug Delivery to CT. The START Program of the Faculty of Medicine, RWTH Aachen (#691405), the MINECO Retos (RyC-2014-13242 and SAF2016-78711), EXOHEP-CM (S2017/BMD-3727), NanoLiver-CM (Y2018/NMT-4949), ERAB (Ref. EA 18/14) AMMF 2018/117, UCM-25-2019, COST Action (CA17112) to FJC, Gilead Research Award 2018. Grant PI16/01126 from the Instituto de Salud Carlos III (ISCIII) co-financed by Fondo Europeo de Desarrollo Regional (FEDER) Una manera de hacer Europa, AECC 2017 Research Grant for Rare and Childhood tumors and Hepacare Project "la Caixa" to MAA. The SFB/TRR57/P04, SFB 1382-403224013/A02, the DFG NE 2128/2-1, MINECO Retos (RyC-2015-17438 and SAF2017-87919R) to YAN. MRM is a recipient of full funded PhD scholarship provided by both German academic exchange service (DAAD) and the Egyptian ministry of higher education (MoHe) (GERLS-German Egyptian Research Long-Term scholarship Program).

View this article online at wileyonlinelibrary.com.

DOI 10.1002/hep4.1495

Potential conflict of interest: Nothing to report.

ARTICLE INFORMATION:

From the [1]Department of Internal Medicine III, University Hospital RWTH Aachen, Aachen, Germany; [2]Department of Immunology, Ophthalmology, and ENT, Complutense University School of Medicine, Madrid, Spain; [3]12 de Octubre Health Research Institute, Madrid, Spain; [4]Department of Therapeutic Chemistry, National Research Center, Giza, Egypt; [5]Department of Genetics, Physiology, and Microbiology, Faculty of Biology, Complutense University, Madrid, Spain; [6]Department of Pathology, Otto-von-Guericke University, Magdeburg, Germany; [7]Diagnostic and Research Center for Molecular BioMedicine, Institute of Pathology, Medical University of Graz, Graz, Austria; [8]Department of Pathology, Neuropathology, and Molecular Pathology, Medical University of Innsbruck, Innsbruck, Austria; [9]Department of Pathobiology, Faculty of Veterinary Medicine, Dutch Molecular Pathology Center, Utrecht University, Utrecht, the Netherlands; [10]Department of Pediatrics, University Medical Center Groningen, University of Groningen, Groningen, the Netherlands; [11]Instituto de Investigación Sanitaria de Navarra, Pamplona, Spain; [12]Hepatology Program, Center for Applied Medical Research, University of Navarra, Pamplona, Spain; [13]Centro de Investigación Biomédica en Red de Enfermedades Hepáticas y Digestivas, Instituto de Salud Carlos III, Madrid, Spain; [14]Nutrition, Metabolism, and Genomics Group, Division of Human Nutrition, Wageningen University, Wageningen, the Netherlands; [15]Howard Hughes Medical Institute, University of Massachusetts Medical School, Worcester, MA.

ADDRESS CORRESPONDENCE AND REPRINT REQUESTS TO:

Francisco Javier Cubero, Ph.D.
Department of Immunology, Ophthalmology, and ENT
Complutense University School of Medicine
c/Doctor Severo Ochoa, 9
Madrid 28040, Spain
E-mail: fcubero@ucm.es
Tel.: +34-91-394-1385
or

Christian Trautwein, M.D.
Department of Internal Medicine III
University Hospital RWTH Aachen
Pauwelsstraße, 30
Aachen 52074, Germany
E-mail: ctrautwein@ukaachen.de
Tel.: +49-241-8080866

The c-Jun N-terminal kinases (JNKs) are evolutionarily conserved mitogen-activated protein kinases (MAPKs) and play an important role in converting extracellular stimuli into a wide range of cellular responses, including inflammatory response, stress response, differentiation, and survival.[4] In tumorigenesis, JNK has been shown to have tumor suppressive function in breast,[5] prostate,[6] lung,[7] and pancreas[8] cancer. However, the pro-oncogenic role for JNK has also been well documented.[9-11] Importantly, JNK has lineage-determinant functions in liver parenchymal cells (LPCs) where it not only favors proliferation of biliary cells but also directly biases biliary cell-fate decisions in bipotential hepatic cells. It has been reported that JNK inhibition delays CCA progression[12] by impeding JNK-mediating biliary proliferation. These data indicate that JNK modulation would be of therapeutic benefit in patients with CCA. Nevertheless, little is known about the cell-type-specific role and mechanism of JNK in biliary overgrowth in order to have a targeted and definite therapy against CCA.

In the present study, we investigated the implications of hepatocyte-defective JNK signaling in experimental carcinogenesis. Unexpectedly, loss of *Jnk1/2* in LPCs inhibited hepatocellular carcinoma (HCC) but triggered biliary epithelium hyperproliferation and features compatible with CCA. Overall, our data uniformly suggest that hepatocytic JNK is pivotal for biliary epithelial hyperproliferation resulting in ducto/cystogenesis.

Materials and Methods

GENERATION OF MICE AND ANIMAL EXPERIMENTS

Albumin (*Alb)-Cre* and *Jnk2*-deficient mice in a C57BL/6J background were purchased from the Jackson Laboratory (Bar Harbor, ME). *Jnk1*$^{\text{locus of X-over P1}(LoxP)/LoxP}$/*Jnk2*$^{-/-}$ (Hepatocyte-specific knockout of *Jnk1* [JNK1$^{\Delta\text{hepa}}$]) mice were created as reported.[13-15] We used male mice for all experiments. For *in vivo* experiments, mice were treated with a daily dose of lapatinib (150 mg/kg weight; n = 7 mice per group) or vehicle (0.5% hydroxypropylmethylcellulose/1% Tween 80) (n = 6) by oral gavage starting at 6 weeks of age over a period of 6 weeks. For small interfering (si)RNA-mediated knockdown experiments, 8-week-old nuclear factor kappa B (NF-κB) essential modulator (NEMO)$^{\Delta\text{hepa}}$/JNK1$^{\Delta\text{hepa}}$ were injected with a dose of 0.2 mg/kg body weight (BW) *siJnk2* or small interfering luciferase (*siLuc*) once per week over a period of 4 weeks. In parallel, lapatinib was given orally to *siJnk2*-treated NEMO$^{\Delta\text{hepa}}$/JNK1$^{\Delta\text{hepa}}$ mice on the same day of the first *siJnk2*- injection. Induction of tumorigenesis was performed by intraperitoneal injection of 25 mg/kg BW of diethylnitrosamine (DEN; Sigma-Aldrich, Munich, Germany) at 14 days of age. Mice were killed 24 weeks later. Vehicle-injected (saline) male mice served as controls.

Animal experiments were carried out according to the German legal requirements and animal protection law and approved by the authority for environment conservation and consumer protection of the state of North Rhine-Westfalia (LANUV; Germany). All strains were crossed on a C57BL/6 background. The mice were housed in the Institute of Laboratory Animal Science at the University Hospital RWTH-Aachen University according to German legal requirements (Animal Welfare Act [DeutschesTierschutzgesetz], Federation of European Laboratory Animal Science Associations [FELASA], Society of Laboratory Animal Science [GV-SOLAS]) under a permit of the Veterinäramt der Städteregion Aachen. All animals received humane care according to the criteria outlined in the Guide for the Care and Use of Animal Models. All organ explants and animal experiments were approved by the local authority for environment conservation and consumer protection of LANUV on the following animal grants: 30034G (AZ-84-02.04.2016.A080) and TVA-11324GZ (AZ-84-02.04.2016.A490).

INTERFERENCE RNA AGAINST *Jnk2* (si*Jnk2*)

The siRNA molecules were purchased from Axolabs GmbH (Kulmbach, Germany) and were chosen due to their ability to specifically target *Jnk2* in mice with mismatches to *Jnk1* (2-18 nucleotides) to increase *in vivo* stability and suppression of the immune-stimulatory properties, as described.[16]

DATA AND SOFTWARE AVAILABILITY

Affymetrix Microarray was performed as described,[17] and data were deposited with the National Center for Biotechnology Information Gene

Expression Omnibus (http://www.ncbi.nlm.nih.gov/geo/) under accession number GSE140498.

STATISTICAL ANALYSIS

All data are expressed as mean ± SEM. Statistical significance was determined by two-way analysis of variance (ANOVA) followed by a Student *t* test or by one-way ANOVA followed by a Newman-Keuls multicomparison test. $P < 0.05$ was considered significant.

Results

COMBINED LOSS OF *Jnk1/2* FUNCTION IN HEPATOCYTES TRIGGERS BILIARY HYPERPROLIFERATION AND DUCTO/CYSTOGENESIS IN AN EXPERIMENTAL MODEL OF CHRONIC LIVER DISEASE

Mice lacking NEMO in LPCs spontaneously develop HCC, rendering these animals an ideal model that perfectly mimics progression of chronic liver disease (CLD) as observed in humans.[18] We previously established that *Jnk1* and *Jnk2* have specific roles for the progression of NEMO$^{\Delta hepa}$-dependent chronic liver injury, indicating that the MAPK genes expressed in liver cells have pivotal functions in cell death and inflammation.[19] We then found that combined activities of *Jnk1* and *Jnk2* specifically in hepatocytes protected against toxic liver injury (CCl_4 and acetaminophen).[15] However, *Jnk1/2* deficiency in hepatocytes increased tumor burden in an experimental model of HCC.[10] Therefore, in the present study we aimed to investigate the definitive contribution of JNK genes to liver cancer.

For this purpose, we generated NEMO$^{\Delta hepa}$/JNK$^{\Delta hepa}$ and their respective controls NEMO$^{\Delta hepa}$ and NEMO$^{floxed\ (f/f)}$ mice (Supporting Fig. S1) and examined the progression of liver disease. At 13 weeks of age, histologic evaluation of NEMO$^{\Delta hepa}$ unveiled the presence of dysplastic nodules, steatohepatitis, and cell death (Supporting Fig. S2A,B). All NEMO$^{\Delta hepa}$/JNK$^{\Delta hepa}$ livers with no external signs of nodules spontaneously showed hyperproliferation of biliary epithelium translated into hepatic ducto/cystogenesis and lymphoid aggregates surrounding these structures (Supporting Fig. S2A,B).

Development of HCC is characteristic of 1-year-old NEMO$^{\Delta hepa}$ mice, visible both macroscopically and histologically. However, most 52-week-old NEMO$^{\Delta hepa}$/JNK$^{\Delta hepa}$ mice displayed no signs of HCC. Here, yellowish coloration of the liver parenchyma was associated with hyperproliferation of biliary epithelial cells and lymphoid cell accumulation. This was much more pronounced than at earlier stages of CLD. Interestingly, histopathological examination of these specimens in two different institutes (Utrecht and Graz) revealed that approximately 33% of 52-week-old JNK$^{\Delta hepa}$ livers presented small cysts while an increased frequency and a higher number of ductular cells were evident in the hepatic parenchyma of all NEMO$^{\Delta hepa}$/JNK$^{\Delta hepa}$, with atypia compatible with CCA (Fig. 1A,B; Table 1).

Moreover, combined JNK1/JNK2 deletion in hepatocytes of NEMO$^{\Delta hepa}$ mice triggered significantly reduced BW and liver weight (LW) compared with NEMO$^{\Delta hepa}$ mice but a similar LW/BW ratio as hepatocyte-specific NEMO-deficient mice (Fig. 1C). Notably, at 13 weeks of age, NEMO$^{\Delta hepa}$/JNK$^{\Delta hepa}$ animals had a significantly increased hepatosomatic ratio compared with NEMO$^{\Delta hepa}$ mice, albeit no differences in BW or LW (Supporting Fig. S2C).

Surprisingly, 1 year-old NEMO$^{\Delta hepa}$/JNK$^{\Delta hepa}$ livers exhibited reduced HCC compared with NEMO$^{\Delta hepa}$ animals (Fig. 1D). In contrast, JNK1/2-deleted NEMO mice displayed ducto/cystogenesis that was much more pronounced than at earlier stages of CLD (Fig. 1B; Supporting Fig. S2D). NEMO$^{\Delta hepa}$/JNK$^{\Delta hepa}$ livers exhibited significantly elevated glutamate dehydrogenase, total bilirubin, alkaline phosphatase, aspartate aminotransferase (AST), and alanine aminotransferase (ALT) levels compared with NEMO$^{\Delta hepa}$ mice, already detectable at 13 weeks (Fig. 1D,E; Supporting Fig. S2D,E). Altogether, these data indicated that deletion of *Jnk1/2* in an experimental model of CLD has pivotal implications in cell death, cholestasis development, and ductular proliferation of cholangiocytes.

ANALYSIS OF THE MICROENVIRONMENT DRIVING MASSIVE BILE DUCT PROLIFERATION IN NEMO$^{\Delta hepa}$/JNK$^{\Delta hepa}$ ANIMALS

Lack of NF-κB activity in hepatocytes triggers spontaneous HCC. In turn, 52-week-old

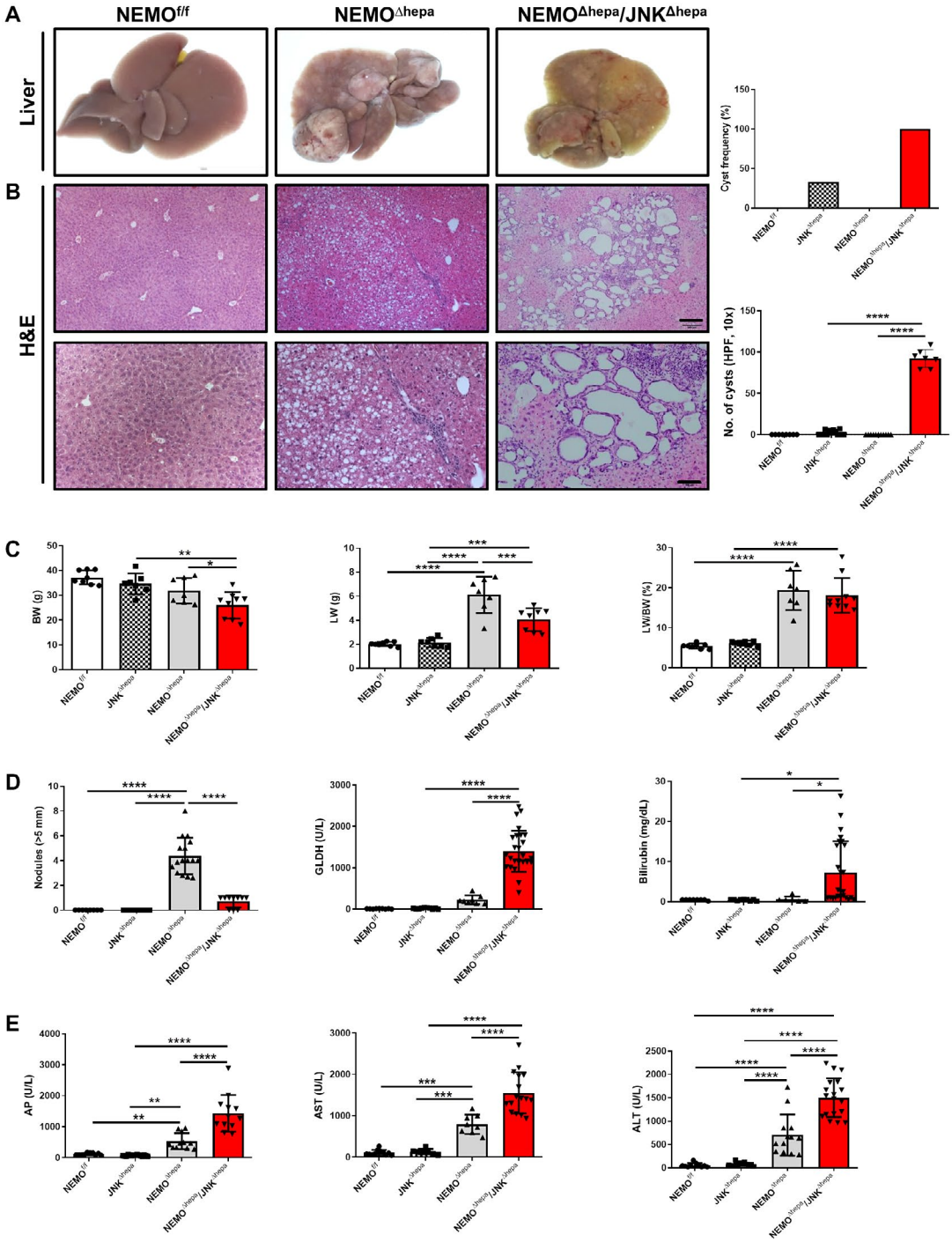

FIG. 1. Deletion of *Jnk1/2* in 52-week-old NEMO$^{\Delta hepa}$ livers triggers cyst formation. (A) Macroscopic view of livers from 52-week-old NEMO$^{f/f}$ (wild type), NEMO$^{\Delta hepa}$, and NEMO$^{\Delta hepa}$/JNK$^{\Delta hepa}$ mice. (B) Representative H&E staining of liver sections of NEMO$^{f/f}$, NEMO$^{\Delta hepa}$, and NEMO$^{\Delta hepa}$/JNK$^{\Delta hepa}$ livers at 52 weeks of age. Different magnifications were used (left). Scale bar 200 μm. Cyst frequency and number of visible microscopic cysts per 10× view field were calculated and graphed (right), magnification is 10× for upper and magnification is 20× for lower. (C) BW (left); LW (center); LW/BW ratio (right). (D) Tumor burden for each individual mouse was characterized by calculating total number of visible tumors >5 mm in diameter per mouse (left); serum levels of GLDH (center); bilirubin (right). (E) Serum levels of AP (left), AST (center), and ALT (right), in 52-week-old NEMO$^{f/f}$, JNK$^{\Delta hepa}$, NEMO$^{\Delta hepa}$, and NEMO$^{\Delta hepa}$/JNK$^{\Delta hepa}$ mice. Data are presented as mean ± SEM. *$P < 0.05$; **$P < 0.01$; ***$P < 0.001$; ****$P < 0.0001$. Abbreviations: AP, alkaline phosphatase; GLDH, glutamate dehydrogenase; H&E, hematoxylin and eosin.

TABLE 1. HISTOPATHOLOGICAL CHARACTERISTICS OF THE DIFFERENT MOUSE GROUPS (SCALE, 0-4)

	$NEMO^{\Delta hepa}$	$NEMO^{\Delta hepa}/JNK^{\Delta hepa}$
Neoplasia	HCC	Cystic cholangioma Mucinous CCA
Anisokaryosis	3.5	2.0
Altered foci	2.0	1.8
Mitosis/HPF (40×)	2.5	1.0
Cellular hypertrophy	3.0	2.5
Dysplasia	3.0	2.5
Oval cell proliferation	1.5	2.5
Portal inflammation	1.0	1.0
Overall inflammation	3.0	3.5
Ductular reaction	1.5	2.0
Apoptosis	1.0	3.0
Fibrosis	3.0	4.0
Steatosis	1.4	0.0
Others	Pale cytoplasm hepatocytes	Massive bile duct proliferation

$NEMO^{\Delta hepa}/JNK^{\Delta hepa}$ mice displayed significantly increased bile duct proliferation. We next investigated liver damage associated with the phenotype of these animals. We first applied terminal deoxynucleotidyl transferase–mediated deoxyuridine triphosphate nick-end labeling (TUNEL) staining, which detects several types of cell death, including necrosis, apoptosis, and necroptosis.[20] $NEMO^{\Delta hepa}$ livers displayed a high percentage of TUNEL-positive cells, while $NEMO^{\Delta hepa}/JNK^{\Delta hepa}$ livers showed significantly increased levels of cell death (Fig. 2A).

Apoptosis and necroptosis are two relevant forms of cell death in the pathogenesis of human and murine liver disease.[21,22] To discriminate between these two types of cell death, we performed immunohistochemistry (IHC) analyses, which revealed significantly higher levels of the apoptosis marker cleaved caspase 3 (CC3) in $NEMO^{\Delta hepa}/JNK^{\Delta hepa}$ livers, especially in cholangiocytes but also in immune infiltrates of these livers (Fig. 2B). We subsequently studied proteins involved in necroptosis, e.g., receptor-interacting serine/threonine-protein kinase 3 (RIPK3) by western blot and IHC, which was found overexpressed in $NEMO^{\Delta hepa}/JNK^{\Delta hepa}$ livers, while no difference in RIPK1 protein expression was found (Fig. 2E; Supporting Fig. S3A).

Cell-cycle dysregulation is characteristic of biliary overgrowth, resulting in CCA. Increased Ki-67-positive and proliferating cell nuclear antigen (PCNA)-positive cells were observed in $NEMO^{\Delta hepa}/JNK^{\Delta hepa}$ frozen and paraffin sections, respectively, the latter further confirmed by immunoblot analysis (Fig. 2C,E; Supporting Fig. S3B). Moreover, the number of transcripts for PCNA and cyclin D1 was up-regulated in $NEMO^{\Delta hepa}/JNK^{\Delta hepa}$ livers (Supporting Fig. S3C). P21 has been shown to induce cell-cycle arrest and promote the DNA repair gene, thus acting as a tumor suppressor.[23,24] Interestingly, we observed p21 overexpression in *Jnk1/2*-deficient $NEMO^{\Delta hepa}$ mice (Fig. 3E). Moreover, oxidative stress in the liver microenvironment has a definitive role in CCA development. We thus measured lipid peroxidation and the antioxidant defense of these animals. Interestingly, strong 4-hydroxynonena immunostaining and catalase depletion (Supporting Fig. S3D,E) in $NEMO^{\Delta hepa}/JNK^{\Delta hepa}$ livers confirmed elevated reactive oxygen species (ROS) production associated with cholangiocellular proliferation.

Hepatic stellate cells (HSCs) are important cells shaping the hepatic microenvironment after liver damage. Hence, HSCs are involved in the high number of α-smooth muscle actin (α-SMA)-positive myofibroblasts and extracellular matrix (ECM) deposition associated with CCA development.[25] Sirius red staining and quantification confirmed strong collagen deposition in $NEMO^{\Delta hepa}/JNK^{\Delta hepa}$ livers (Fig. 2D; Supporting Fig. S4A). Furthermore, collagen type I alpha 1 (Col1A1) and α-SMA were dramatically overexpressed in $NEMO^{\Delta hepa}/JNK^{\Delta hepa}$ liver protein lysates (Fig. 2E) and were associated with significantly increased transcripts of *col IA1*, matrix metalloproteinase (*mmp*)*7/9/12,* and tissue inhibitor of metalloproteinase (*timp*)*1* (Supporting Fig. S4B,C). Cytokine-mediated tissue fibrosis was also measured, and levels of monocyte chemoattractant protein 1 (*mcp1*), tumor necrosis factor (*tnf*), interleukin (*il*)*1β*, and regulated upon activation, normal T cell expressed, and secreted (*rantes*) were significantly up-regulated in $NEMO^{\Delta hepa}/JNK^{\Delta hepa}$ mice (Supporting Fig. S4D,E). Altogether, these data suggest that fibrogenesis and unresolved inflammation are involved in CCA development in the $NEMO^{\Delta hepa}/JNK^{\Delta hepa}$ context while HCC-related tumorigenesis is diminished as confirmed by low glutamine synthase expression (Supporting Fig. S5A).

$NEMO^{\Delta hepa}/JNK^{\Delta hepa}$ LIVERS EXHIBIT TYPICAL FEATURES OF HUMAN CCA

Immunohistochemical analysis revealed that many ductules were composed of creatine kinase

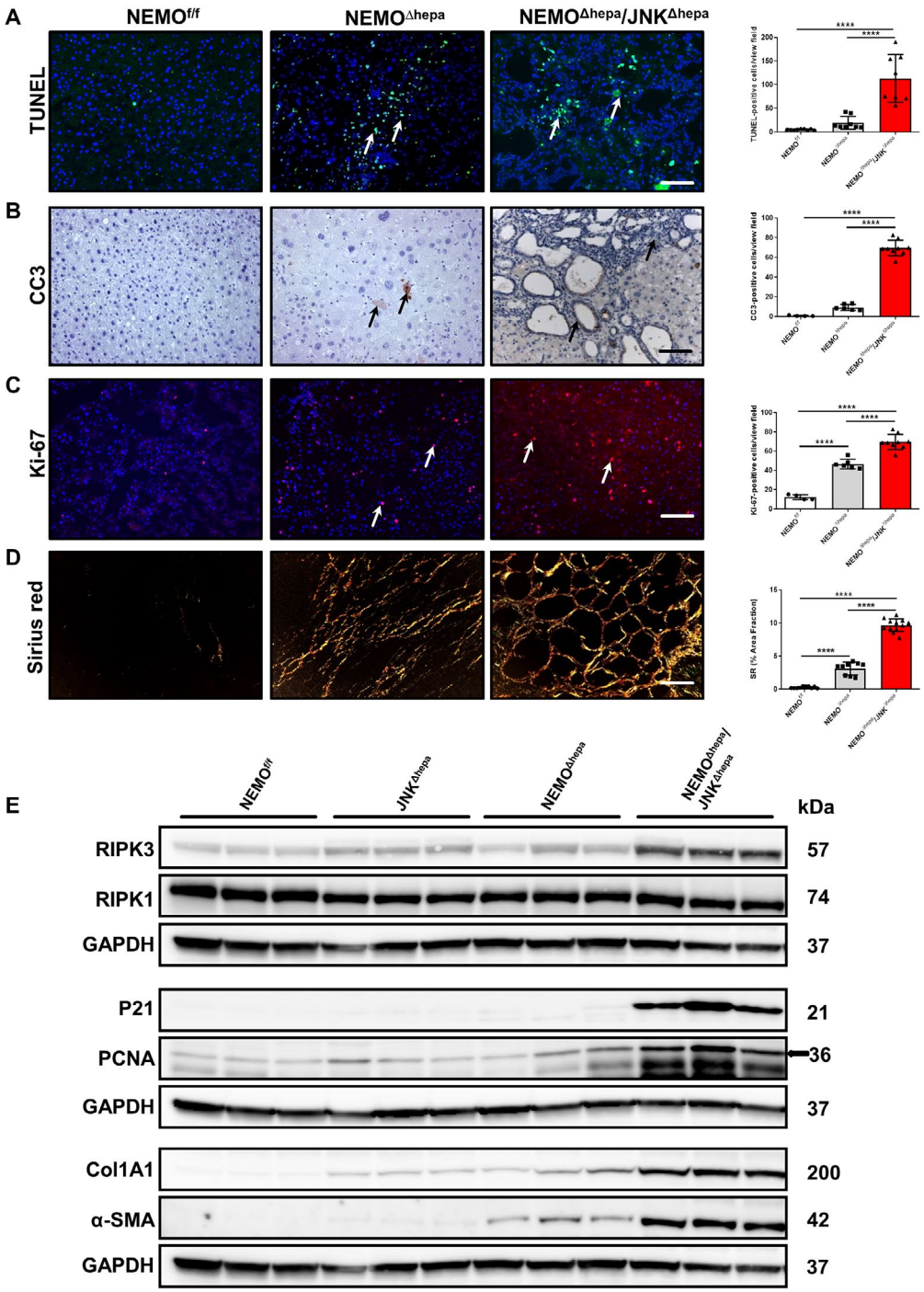

FIG. 2. Characterization of cell death, cell proliferation, and collagen deposition in 52-week-old NEMO$^{\Delta hepa}$/JNK$^{\Delta hepa}$ mice. (A) Representative TUNEL staining of liver sections of NEMO$^{f/f}$, NEMO$^{\Delta hepa}$, and NEMO$^{\Delta hepa}$/JNK$^{\Delta hepa}$ livers at 52 weeks of age (left). TUNEL-positive cells were quantified and graphed (right). (B) Representative IHC staining for CC3 of the same livers (left). CC3-positive cells were quantified and graphed (right). (C) Immunofluorescent staining for Ki-67 of liver cryosections from the same livers (left). Ki-67-positive cells were quantified and graphed (right). (D) Representative sirius red staining of paraffin sections from the indicated genotypes (left). Quantification of the positive sirius red area fraction was performed with Image J and graphed (right). (A-D) Scale bars, 200 μm. Arrows (→) indicate positive cells. Data are presented as mean ± SEM; ****$P < 0.0001$. (E) Protein levels of α-SMA, Col1A1, PCNA, p21, RIPK1, and RIPK3 from whole-liver extracts of 52-week-old NEMO$^{f/f}$, JNK$^{\Delta hepa}$, NEMO$^{\Delta hepa}$, and NEMO$^{\Delta hepa}$/JNK$^{\Delta hepa}$ mice were analyzed by western blot with the indicated antibodies. GAPDH was used as a loading control.

(CK)19-positive cells. In fact, NEMO$^{\Delta hepa}$/JNK$^{\Delta hepa}$ cystic and CCA-like structures exhibited CK19-positive staining that was corroborated by dramatically elevated CK7/19 messenger RNA (mRNA) expression in these livers (Fig. 3A,D). NEMO$^{f/f}$ had regular small bile ducts, and NEMO$^{\Delta hepa}$ exhibited mild to

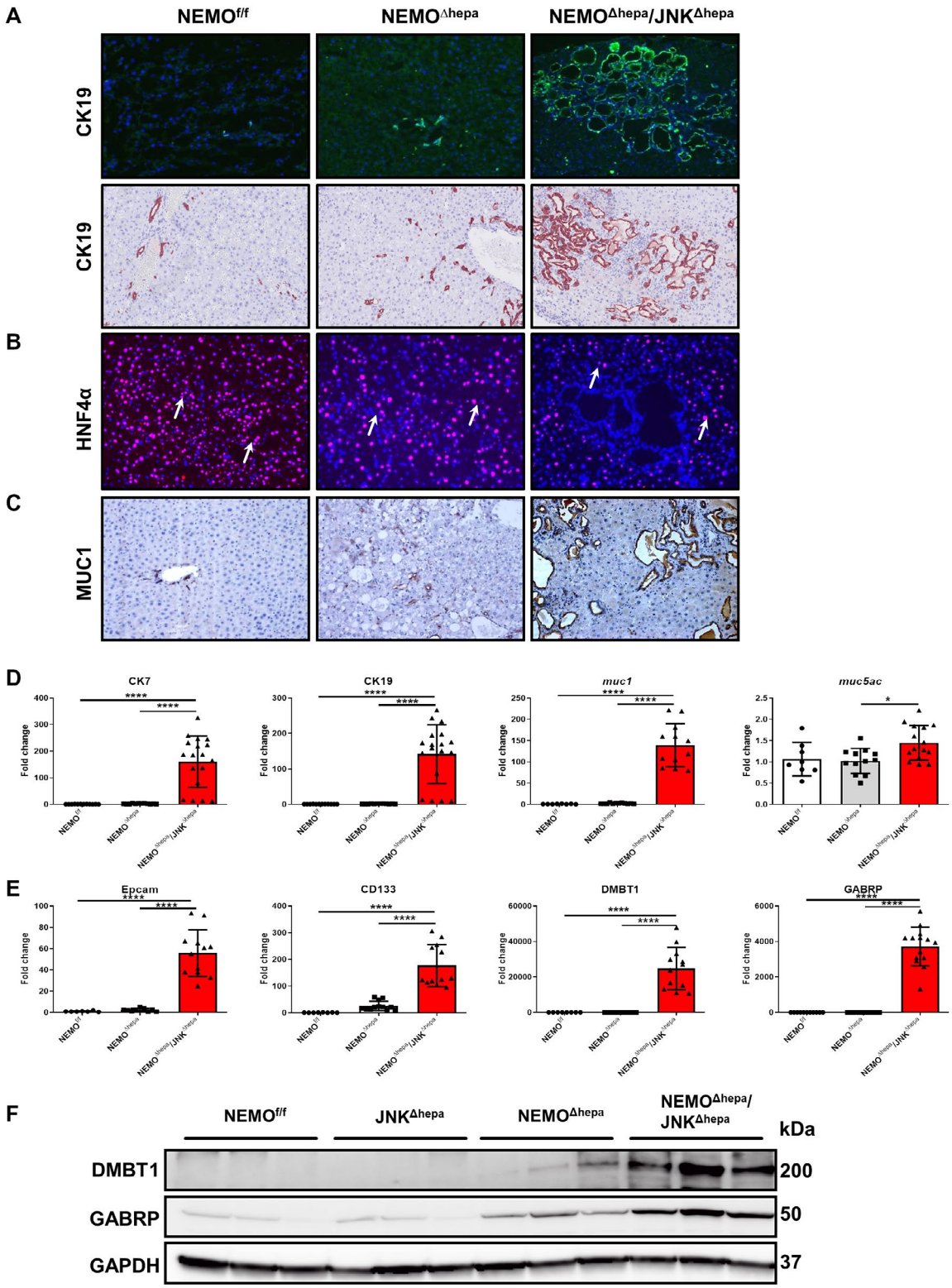

FIG. 3. Loss of *Jnk1/2* in NEMO$^{\Delta hepa}$ hepatocytes triggers cholangiocellular proliferation. (A) Representative IF for CK19 of liver cryosections was performed in 52-week-old NEMO$^{f/f}$, NEMO$^{\Delta hepa}$, and NEMO$^{\Delta hepa}$/JNK$^{\Delta hepa}$ livers (upper panel). IHC staining for CK19 reveals densely packed cholangiocellular proliferates with a tubular growth pattern mimicking morphologic features of well-differentiated human CCA (lower panel), magnification is 20×. (B) Representative IF staining for HNF-4α of the same livers, magnification is 20×. (C) Representative IHC staining for Muc1, magnification is 20×. (D) mRNA expression analysis of CK7 (left), CK19, and *muc1* (center) and *muc5ac* (right) was quantified by qRT-PCR in the same livers. (E) mRNA expression analysis of Epcam (left), CD133 and DMBT1 (center), and GABRP (right) was quantified by qRT-PCR of samples taken from NEMO$^{f/f}$, NEMO$^{\Delta hepa}$, and NEMO$^{\Delta hepa}$/JNK$^{\Delta hepa}$ livers killed at 52 weeks. (F) Protein expressions of GABRP and DMBT1 from whole-liver extracts of 52-week-old NEMO$^{f/f}$, JNK$^{\Delta hepa}$, NEMO$^{\Delta hepa}$, and NEMO$^{\Delta hepa}$/JNK$^{\Delta hepa}$ mice were analyzed by western blot with the indicated antibodies. GAPDH served as loading control. Data are presented as mean ± SEM. $^{*}P < 0.05$; $^{****}P < 0.0001$. Abbreviations: CD, cluster of differentiation; Epcam, epithelial cell adhesion molecule; IF, immunofluorescence.

moderate ductular proliferates similar to a ductular reaction in humans. Noticeably, livers of NEMO$^{\Delta hepa}$/JNK$^{\Delta hepa}$ mice displayed cholangiocellular proliferates with a tubular architecture resembling the morphology of human well-differentiated CCA, highlighted by a strong-positive CK19 signal. In contrast, hepatocyte nuclear factor (HNF)-4α staining was characteristic of pericystic areas and hepatocytes of NEMO$^{\Delta hepa}$ and NEMO$^{f/f}$ livers (Fig. 3B). Cells containing cytoplasmic mucin (MUC) granules are common in CCA tissues.[26] Thus, we assessed the expression of MUC1 and MUC5AC, which are closely related to dedifferentiation, infiltrative growth pattern, and patient survival.[26] Whereas MUC1 staining was limited to areas of ductogenesis or oval cell reaction in NEMO$^{\Delta hepa}$ livers, it was very strong in cysts of NEMO$^{\Delta hepa}$/JNK$^{\Delta hepa}$ livers, which were associated with significantly increased *muc1* and *muc5ac* mRNA levels in these mice (Fig. 3C,D).

High expression of cholangiocyte markers, including cluster of differentiation (*cd*)*133* and expression of CCA/tumor-enriched markers, including epithelial cell adhesion molecule (*epcam*), deleted in malignant brain tumors 1 (*dmbt1*), and gamma-aminobutyric acid A receptor, pi (*gabrp*),[27] together with the accumulation of transcription factor SOX 9 (SOX-9)-positive cells (Fig. 3E,F; Supporting Fig. S5B) suggest that loss of *Jnk1/2* function in hepatocytes promotes the shift from HCC to CCA in this experimental model of CLD.

ADMINISTRATION OF DEN TO JNK$^{\Delta hepa}$ MICE TRIGGERS HEPATIC DUCTO/CYSTOGENESIS WITHOUT HEPATOCARCINOGENESIS

To validate the relevance of *Jnk1/2* in mediating the shift from HCC to CCA, we applied a second model of carcinogenesis, the DEN model. Previously, Das and colleagues,[10] using mice with compound deficiency of *Jnk1/2* in hepatocytes, demonstrated that the JNK genes possess tumor-suppressing roles in liver carcinogenesis that depend on the cell types of the liver. Additionally, we showed that hepatocyte-specific *Jnk1/2* knockout female and male mice have no phenotype affecting the correct function of the liver.[15] These previous results are confirmed in the present study in a larger pool of animals ranging from 13 to 52 weeks of age (Supporting Figs. S6A-D and S7A-D). However, approximately 33% of these mice from week 30 of age histologically displayed tumors resembling human CCA in their liver parenchyma that did not affect liver function (Fig. 1A,B; Supporting Fig. S7A-D).

JNK$^{\Delta hepa}$ mice were challenged with the carcinogen DEN. Interestingly, these mice exhibited jaundice and the liver was yellowish albeit with decreased tumor load (Supporting Fig. S8A). The LW/BW ratio was significantly decreased in JNK$^{\Delta hepa}$ compared with JNK$^{f/f}$ mice (Supporting Fig. S8B). Histologic evaluation performed by two blinded pathologists demonstrated the presence of cystogenesis and cholangioma-like structures in liver parenchyma accompanied by strong infiltration of immune cells (Fig. S8C). The analysis of serum transaminases in JNK$^{\Delta hepa}$ demonstrated decreased ALT and AST levels in these animals (Fig. S8D,E). These results indicated that JNK1 and JNK2 might influence cell fate during liver tumorigenesis.

To further analyze the differences between both animal models, age progression versus chemically induced HCC, we performed a microarray analysis (Supporting Fig. S9A,B). Interestingly, *dmbt1*, *muc1*, *gabrp,* and immunoglobulin heavy chain (gamma polypeptide) (*igh*g)*2b* were commonly up-regulated in *Jnk1/2*-deficient NEMO$^{\Delta hepa}$ mice and *Jnk1/2*-deficient mice challenged with DEN, indicating that epithelial–mesenchymal transition (EMT) might be modulated through a JNK-dependent mechanism.

Next, we analyzed total common up-regulated and down-regulated genes in NEMO$^{\Delta hepa}$/JNK$^{\Delta hepa}$ versus JNK$^{\Delta hepa}$ + DEN, which were the majority compared to specific changes of each experimental model (Supporting Fig. S9C,D). Heat map analysis of these genes showed up-regulation of genes related to CCA, like *dmbt1*, *muc1*, *gabrp*, and matrix deposition, including *timp1* and *mmp12*, and down-regulation of serpines, which are often implicated in HCC development (Fig. 4A). Altogether, these data reinforce the notion that the JNK signaling pathway modulates cell fate during liver carcinogenesis.

OVEREXPRESSION OF THE IL-6/SIGNAL TRANSDUCER AND ACTIVATOR OF TRANSCRIPTION 3 PATHWAY IS CHARACTERISTIC FOR NEMO$^{\Delta hepa}$/JNK$^{\Delta hepa}$ LIVERS

Cytokines play an important role during carcinogenesis by shaping the inflammatory microenvironment toward malignant transformation. In particular, IL-6 has been demonstrated to have an integral role in CCA biology and other cancers as a growth and survival factor.[28] Under physiologic conditions, IL-6 through a Janus kinase (JAK)/signal transducer and activator of transcription (STAT) 3 pathway induces expression of suppressor of cytokine signaling 3 (SOCS3), accelerating inflammation, cell growth, and tumor formation. We found overexpression of *il6*, *il6* receptor (*il6r*), and *socs3* mRNA as well as other IL-6 family members, including LIF IL-6 family cytokine (*lif*) and oncostatin M (*osm*) (Fig. 4B,C; Supporting Fig. S10A). OSM has recently been identified as an important regulator of the EMT/cancer stem cell plasticity program that promotes tumorigenic properties.[29] *Osm* was significantly increased in NEMO$^{\Delta hepa}$/JNK$^{\Delta hepa}$ livers.

Concomitantly, high phosphorylated STAT3 (pSTAT3) levels were evident in NEMO$^{\Delta hepa}$/JNK$^{\Delta hepa}$ compared with NEMO$^{\Delta hepa}$ livers (Fig. 4D; Supporting Fig. S10B), indicating that this pathway is strongly activated in our murine model.

THE EGF-Raf-MEK-ERK1/2 PATHWAY IS OVEREXPRESSED IN NEMO$^{\Delta hepa}$/JNK$^{\Delta hepa}$ ANIMALS

Activation of Notch and Wnt signaling pathways stimulates proliferation of the hepatic progenitor cell compartment. In particular, NOTCH signaling is implicated in the commitment toward the cholangiocyte fate, while WNT can trigger differentiation toward the hepatocyte lineage.[30] Therefore, we first assessed the relevance of Notch-1 (A6) in NEMO$^{\Delta hepa}$/JNK$^{\Delta hepa}$ livers. Interestingly, A6 staining was positive in clusters of immune cells in NEMO$^{\Delta hepa}$ livers. NEMO$^{\Delta hepa}$/JNK$^{\Delta hepa}$ livers exhibited increased Notch-1 expression throughout the liver parenchyma (Fig. 5A). In fact, other family members, including *Notch2,* were significantly up-regulated or had a tendency toward increased mRNA levels in NEMO$^{\Delta hepa}$/JNK$^{\Delta hepa}$ livers (Fig. 5C; Supporting Fig. S11A-F). However, no differences in β-catenin expression between NEMO$^{\Delta hepa}$ and NEMO$^{\Delta hepa}$/JNK$^{\Delta hepa}$ livers were observed (Fig. 5D). Of note, JNK1/2-knockout mice had reduced phosphorylation of β-catenin, indicating that JNK is necessary for β-catenin phosphorylation, as suggested.[31]

The epidermal growth factor receptor (EGFR) family includes erythroblastic oncogene B (ERBB)1, 2, 3, and 4, with ERBB1/EGFR and ERBB2/human epidermal growth factor receptor 2 (HER2) (Neu in rodents) being frequently implicated in the multistep carcinogenesis of CCA.[32] Specifically, HER2 is a well-described predictive biomarker for positive anti-HER2 therapy response in breast and gastric cancer and, lately, in CCA.[33,34] Our first results showed dramatically increased ErbB2 protein and mRNA levels in livers of NEMO$^{\Delta hepa}$/JNK$^{\Delta hepa}$ compared with NEMO$^{\Delta hepa}$ hepatic tissue (Fig. 5B-D). Interestingly, we also found increased expression of the EGFR ligand *egf* (Fig. 5C). Consistently, the levels of EGFR phosphorylation (pEGFR) were markedly elevated in the livers of NEMO$^{\Delta hepa}$/JNK$^{\Delta hepa}$ mice (Fig. 5D).

The rapidly accelerated fibrosarcoma (RAF)-mitogen-activated protein kinase kinase (MEK)-extracellular signal-regulated kinase (ERK) transduction pathway is a key signaling cascade that regulates cellular proliferation, differentiation, and apoptosis and is frequently dysregulated in HCC[35] and in biliary tract cancer.[36] Binding of EGF to EGFR triggers its tyrosine kinase activity downstream signaling leading to the end phosphorylation of MEK1/2 and ERK1/2, with translocation of ERK to the nucleus and expression of genes related to proliferation. Increased phosphorylation (i.e., activation) of RAF, MEK1/2, and ERK/2 was

found in NEMO$^{\Delta hepa}$/JNK$^{\Delta hepa}$ mice (Fig. 5D) associated with biliary overgrowth. These results were further corroborated in livers of 13-week-old mice (Supporting Fig. S12), indicating that the RAF-MEK-ERK pathway was constitutively activated at early stages of cholangiocarcinogenesis.

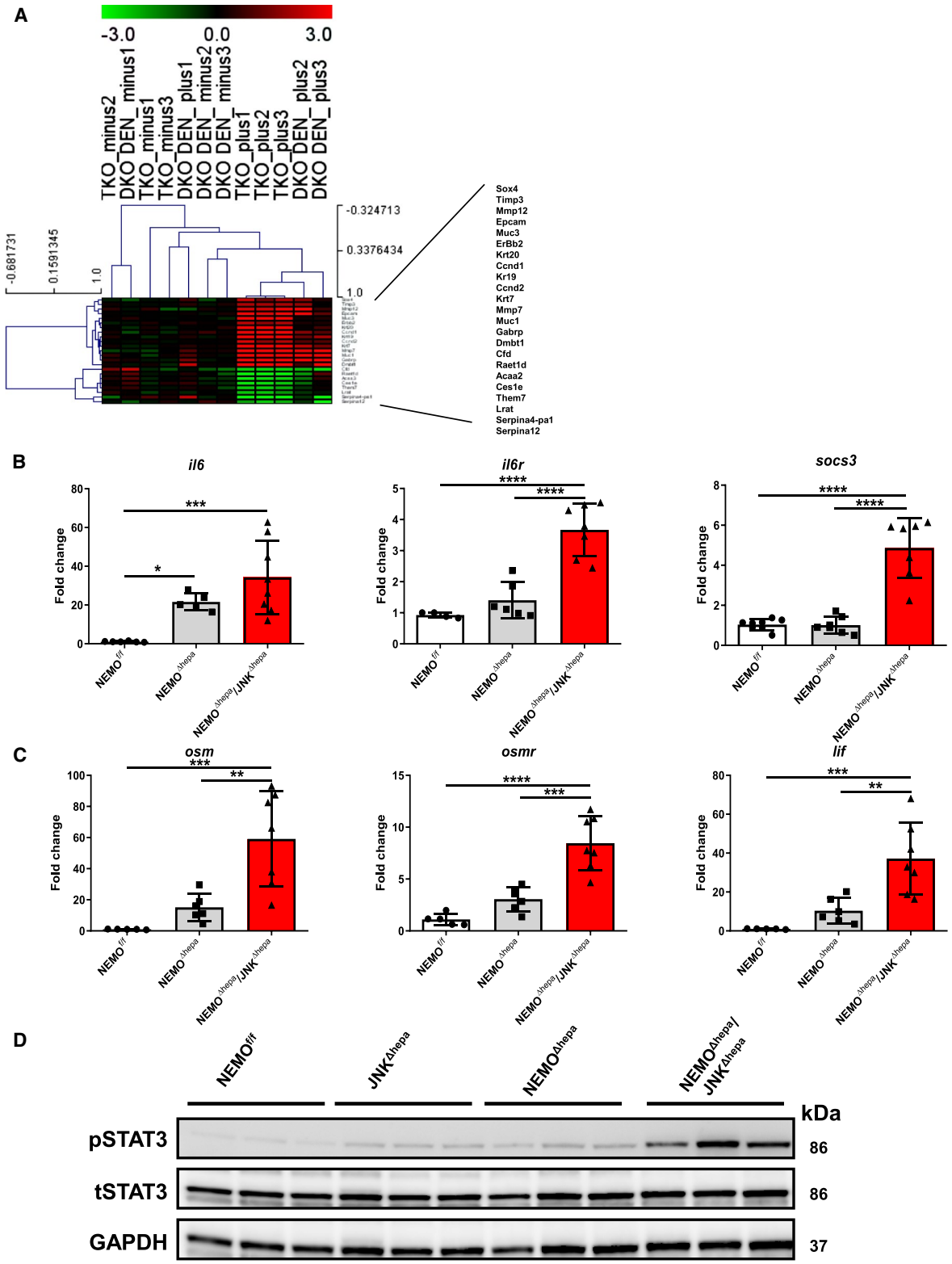

FIG. 4. The IL-6/STAT3 pathway is pivotal in biliary cell proliferation during liver carcinogenesis. (A) Gene array analysis was performed in 8-week-old NEMO$^{\Delta hepa}$/JNK$^{f/f}$ and NEMO$^{\Delta hepa}$/JNK$^{\Delta hepa}$ livers in addition to 26-week-old wild type and JNK$^{f/f}$ and JNK$^{\Delta hepa}$ livers challenged with DEN. Correlation of the fold induction of gene expression in liver is shown. Log2 expression values of the individual mice were divided by the mean of the NEMO$^{\Delta hepa}$/JNK$^{\Delta hepa}$ mice. Log ratios were saved in a .txt file and analyzed with the Multiple Experiment Viewer. Top up-regulated and down-regulated target substrates are shown (red, up-regulated; green, down-regulated; n = 3, 3.0< fold change >3.0). (B) mRNA expression analysis of *il6* (left); *il6r* (center), *and socs3* (right). (C) mRNA expression analysis of *osm* (left), *osmr* (center), and *lif* (right) was quantified by qRT-PCR of samples taken from NEMO$^{f/f}$, NEMO$^{\Delta hepa}$, and NEMO$^{\Delta hepa}$/JNK$^{\Delta hepa}$ livers killed at 52 weeks. (D) Protein expression levels of STAT3 and pSTAT3 from whole-liver extracts of 52-week-old NEMO$^{f/f}$, JNK$^{\Delta hepa}$, NEMO$^{\Delta hepa}$, and NEMO$^{\Delta hepa}$/JNK$^{\Delta hepa}$ mice were analyzed by western blot with the indicated antibodies. GAPDH served as loading control. Abbreviations: DKO, JNK1$^{f/f}$/JNK2$^{-/-}$ + DEN; LIF, leukemia inhibitory factor; osmr, oncostatin M receptor; TKO, NEMO$^{\Delta hepa}$/JNK$^{\Delta hepa}$.

LAPATINIB TREATMENT PREVENTS BILIARY EXPANSION AND DUCTO/CYSTOGENESIS IN NEMO$^{\Delta hepa}$/JNK$^{\Delta hepa}$ MICE

Our data strongly indicate the EGFR-HER2 pathway being involved in biliary cell hypergrowth and cholangiocarcinogenesis in NEMO$^{\Delta hepa}$/JNK$^{\Delta hepa}$ livers. Lapatinib is a dual EGFR2/HER2 tyrosine kinase inhibitor (TKI) targeting both EGFR and HER2.[37,38] It successfully inhibited the growth of HER-overexpressing breast cancer cells in culture and in tumor xenografts.[39] Taking into consideration the promising therapeutic option of lapatinib, we subsequently explored the potential beneficial effect of this dual TKI in our model of cholangiocellular proliferation.

Lapatinib was administered daily by oral gavage for 6 weeks in NEMO$^{f/f}$, NEMO$^{\Delta hepa}$, and NEMO$^{\Delta hepa}$/JNK$^{\Delta hepa}$ mice (Fig. 6A). The TKI did not cause any relevant histopathological or serum biochemistry alterations to NEMO$^{f/f}$ or NEMO$^{\Delta hepa}$ animals (Fig. 6B). However, lapatinib treatment of NEMO$^{\Delta hepa}$/JNK$^{\Delta hepa}$ mice resulted in a significant reduction of cyst-like structures (Fig. 6B). Lapatinib also significantly reduced serum AST and ALT levels in NEMO$^{\Delta hepa}$/JNK$^{\Delta hepa}$ compared with NEMO$^{f/f}$ and NEMO$^{\Delta hepa}$ animals (Fig. 6C).

Next, the impact of lapatinib on EGFR/HER2 signaling was tested by investigating the downstream RAF-MEK-ERK pathway below EGFR/HER2. Decreased activation of EGFR and abrogation of RAF, MEK, and ERK signaling pathways were found in lapatinib-treated livers compared with vehicle-administrated NEMO$^{\Delta hepa}$/JNK$^{\Delta hepa}$ livers (Fig. 6D). These results suggest that lapatinib successfully decreases EGFR-HER2 signaling and functionally links inhibition of this pathway with biliary overgrowth in NEMO$^{\Delta hepa}$/JNK$^{\Delta hepa}$ livers.

COMBINED JNK1/JNK2 DELETION IS ESSENTIAL FOR HYPERPROLIFERATION OF BILE DUCTS

Our data were generated in global JNK2$^{-/-}$ mice. Hence, we aimed to distinguish if hepatocytic or nonparenchymal JNK2 function is essential to direct bile duct proliferation. We applied our recently developed hepatocyte-specific *Jnk2* siRNA (*siJnk2*) protocol using lipid nanoparticles[16]; *siLuc* served as controls. We included 6- to 8-week-old untreated floxed NEMO$^{f/f}$/JNK$^{f/f}$, *siLuc*-treated NEMO$^{\Delta hepa}$/JNK1$^{\Delta hepa}$, and *siJnk2*-challenged NEMO$^{\Delta hepa}$/JNK1$^{\Delta hepa}$ mice in this analysis. In parallel, animals were treated with vehicle or lapatinib.

Interestingly, *Jnk2* knockdown in hepatocytes triggered massive biliary cyst formation in livers of vehicle-treated NEMO$^{\Delta hepa}$/JNK1$^{\Delta hepa}$ animals compared with siLuc-NEMO$^{\Delta hepa}$/JNK1$^{\Delta hepa}$ and untreated floxed NEMO$^{f/f}$/JNK$^{f/f}$ mice (Supporting Fig. S13A). These results demonstrate that combined *Jnk1/2* deletion in hepatocytes is responsible for directing biliary hyperproliferation in this model. Additionally, lapatinib treatment successfully reduced liver cystogenesis and significantly ameliorated serum transaminases in NEMO$^{\Delta hepa}$/JNK1$^{\Delta hepa}$ + *siJnk2* livers, confirming the efficacy of this TKI in experimental biliary cystogenesis (Supporting Fig. S13B-D).

Discussion

Hyperplasia of the biliary epithelia with variable atypia in cystic bile ducts may give rise to malignant transformation leading to intrahepatic CCA for which an enormous unmet clinical and research need exists. CCA is an epithelial neoplasm derived from

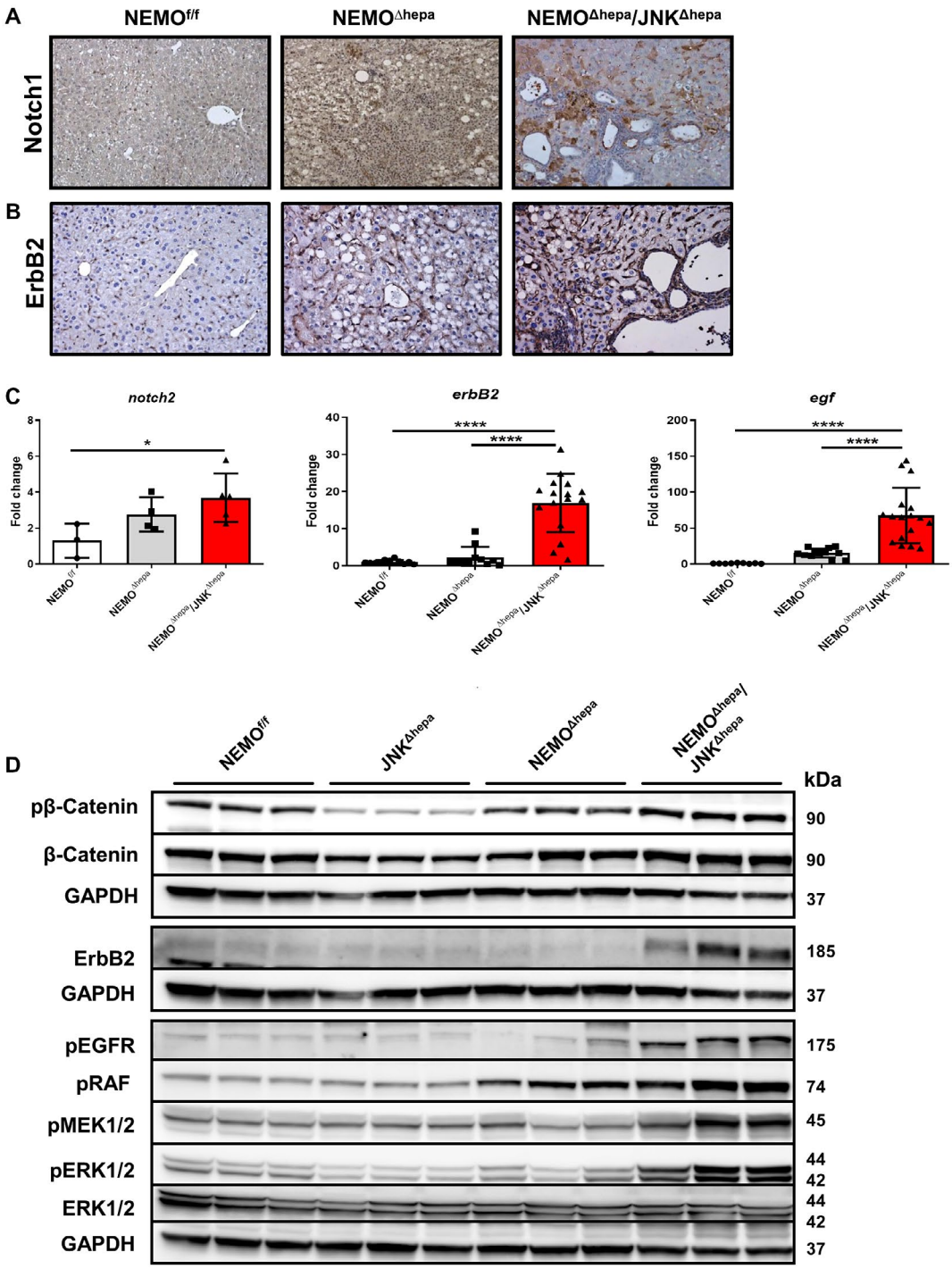

FIG. 5. Activation of EGF-EGFR-RAF-MEK1/2-ERK1/2 is distinctive of NEMO$^{\Delta hepa}$/JNK$^{\Delta hepa}$ mice. (A) Representative IHC for NOTCH-1 staining of liver sections of 52-week-old NEMO$^{f/f}$, NEMO$^{\Delta hepa}$, and NEMO$^{\Delta hepa}$/JNK$^{\Delta hepa}$ livers, magnification is 20×. (B) Representative IHC for ErbB2 staining of liver sections of the same livers. (C) mRNA expression analysis of *notch-2* (left), *erbB2* (center), and *egf* (right) was quantified by qRT-PCR of samples taken from NEMO$^{f/f}$, NEMO$^{\Delta hepa}$, and NEMO$^{\Delta hepa}$/JNK$^{\Delta hepa}$ mice killed at 52 weeks. Data are presented as mean ± SEM. *$P < 0.05$; ****$P < 0.0001$. (D) Protein expressions of phospho-β-catenin, β-catenin, ErbB2, phospho-EGFR, phospho-RAF, phospho-MEK1/2, phospho-ERK1/2, and total ERK1/2 from whole-liver extracts of 52-week-old NEMO$^{f/f}$, JNK1$^{\Delta hepa}$/JNK2$^{-/-}$, NEMO$^{\Delta hepa}$, and NEMO$^{\Delta hepa}$/JNK$^{\Delta hepa}$ mice were analyzed by western blot with the indicated antibodies. GAPDH served as loading control. Abbreviation: phospho, phosphorylated.

primary and secondary bile tracts and accounts for 5%-10% of primary liver cancer, the incidence and mortality of which are steadily increasing. The 5-year survival of patients with CCA remains unacceptably low, and survival has not dramatically improved in the past 20 years.[40] This is in part due to a lack of

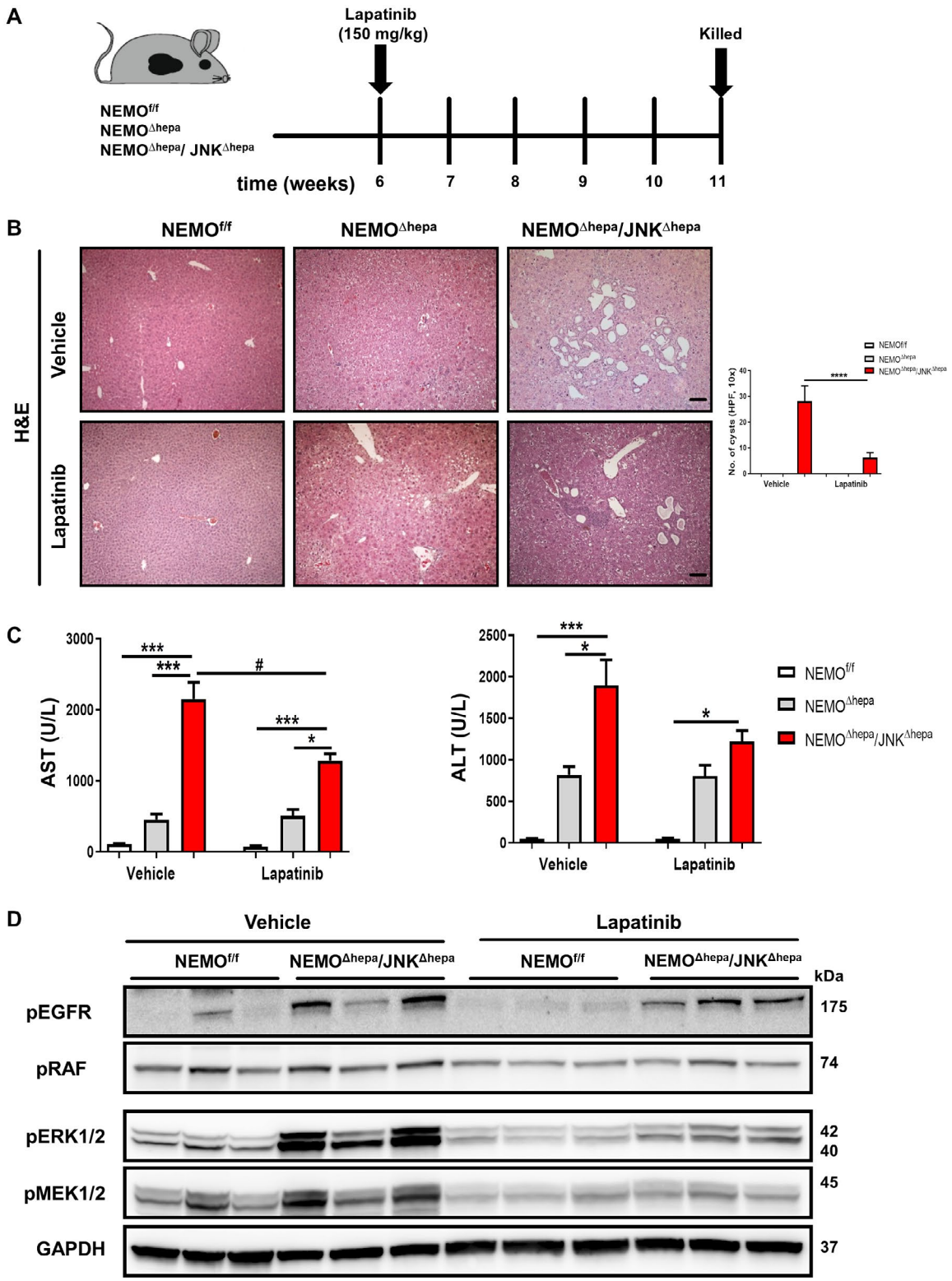

FIG. 6. Lapatinib, a dual tyrosine kinase inhibitor, protects against hyperbiliary proliferation in 52-week-old NEMO$^{\Delta hepa}$/JNK$^{\Delta hepa}$ animals. (A) Experimental design of lapatinib (150 mg/kg BW) or vehicle administration to 6-week-old NEMO$^{f/f}$, NEMO$^{\Delta hepa}$, and NEMO$^{\Delta hepa}$/JNK$^{\Delta hepa}$ mice. (B) Representative H&E staining of liver sections of NEMO$^{f/f}$, NEMO$^{\Delta hepa}$, and NEMO$^{\Delta hepa}$/JNK$^{\Delta hepa}$ livers treated with either vehicle or lapatinib for 6 weeks (left), magnification is 10×. Number of visible microscopic cysts per 10× view field were calculated and graphed (right). (C) Serum levels of AST and ALT, in NEMO$^{f/f}$, NEMO$^{\Delta hepa}$, and NEMO$^{\Delta hepa}$/JNK$^{\Delta hepa}$ mice after 6 weeks of lapatinib treatment. Data are presented as mean ± SEM. $^{*}P < 0.05$, $^{***}P < 0.001$, $^{\#}P < 0.05$ (intergroup). (D) Levels of phospho-ERK1/2, phospho-MEK1/2, phospho-RAF, and phospho-EGFR from whole-liver extracts of the indicated genotypes treated with vehicle or lapatinib were analyzed by western blot with the indicated antibodies. GAPDH served as loading control. Abbreviations: H&E, hematoxylin and eosin; phospho, phosphorylated.

understanding of the pathophysiologic mechanisms underlying CCA. Because biliary tract cancer is often diagnosed late, the success of the only curative procedure (surgical resection) is limited, and the lack of biomarkers or diagnostic tools that would lead to early diagnosis is a matter of concern.[41]

A recent study[12] opened a Pandora´s box for therapeutic options targeting the JNK signaling pathway, a major regulator of cell proliferation, against CCA. Earlier, several studies confirmed the critical role of the JNK signaling pathway in liver cancer.[10,19,42-44] At present, little is known on the role of JNK in directing differentiation of LPCs and more specifically of bipotential hepatic cells not only in liver homeostasis but also following liver injury.

We first focused on the specific roles of the *Jnk* genes in the progression of experimental chronic liver disease using NEMO mice and showed how *Jnk1* or *Jnk2* tipped the balance toward HCC or necroinflammation, respectively.[19] We later demonstrated that combined *Jnk1/2* deletion in hepatocytes triggers more severe liver injury, inflammation, and progression after toxic liver injury.[15]

Thus, we next sought to investigate the consequences of hepatocytic *Jnk1/2* ablation in liver parenchymal proliferation and growth in experimental HCC. For this purpose, we generated NEMO$^{\Delta hepa}$/JNK$^{\Delta hepa}$ mice, which displayed reduced tumor burden, despite the fact that they had signs of jaundice and hyperbilirubinemia, compared to NEMO-deficient mice developing HCC.[18] Remarkably, *Jnk1/2*-deleted NEMO$^{\Delta hepa}$ livers exhibited hyperproliferation of the biliary epithelium, forming cyst-like structures compatible with cholangioma or malignant CCA, as assessed by two independent pathologists (Table 1).

These livers were characterized by cell death, inflammatory microenvironment, and ECM deposition. Necroptosis-associated hepatic cytokine microenvironment induces the shift from HCC to CCA development.[22] NEMO$^{\Delta hepa}$/JNK$^{\Delta hepa}$ livers display considerable CC3 staining and RIPK3 protein levels, triggering exacerbated compensatory proliferation of LPCs, which are associated with increased ROS production and failure of the antioxidant defense.

Moreover, deposition of ECM and periductural/pericystic scar formation was a prominent feature in NEMO$^{\Delta hepa}$/JNK$^{\Delta hepa}$ livers. A unique characteristic of CCA is the presence of cancer-associated fibroblasts (CAFs) surrounded by numerous immune cells.[41] CAFs promote the secretion of chemokines/cytokines including EGF in CCA cell lines.[45] Moreover, TNF might be another important culprit in CCA development, as suggested.[12]

In parallel with proliferating hepatocytes and a marked expansion of the biliary epithelium, the liver parenchyma of NEMO$^{\Delta hepa}$/JNK$^{\Delta hepa}$ animals was positive for CK19 and SOX-9 and negative for HNF-4α. Moreover, we found increased expression of mucin genes. Considering that CCA tissues are characterized by the presence of mucin-secreting cells, this finding further supports the CCA diagnosis.[46] Interestingly, analysis of gene expression showed the occurrence of CCA/epithelial-transformed neoplasia-enriched markers, including *Dmbt1* and *Gabrp,* not only in NEMO$^{\Delta hepa}$/JNK$^{\Delta hepa}$ liver but also in a second model of liver carcinogenesis, the DEN model. Confirmation in the two models suggests that CCA development relies on *Jnk1/2* combined function in hepatocytes but is independent of NF-κB activity in LPCs. Moreover, microarray studies highlighted the pivotal role of *Jnk1/2* in modulating cell fate by promoting hepatocarcinogenesis and under-regulating cascades linked with cholangiocarcinogenesis. Our data undoubtedly indicate that loss of *Jnk1/2* function promoted CCA in both experimental CLD and chemically induced HCC.

Jnk1/2-deleted NEMO livers exhibited strong expression of NOTCH-1/A6 and *Notch-2* and a clear tendency toward increased expression of Notch signaling pathway effectors. These results are consistent

with evidence from mouse studies, suggesting that NOTCH and WNT/β-catenin are key drivers of CCA development. Specifically, NOTCH-1, -2, and -3 were shown to be overexpressed in human cholangiocellular injury.[47] In contrast, no differences in β-catenin expression between NEMO$^{\Delta hepa}$ and NEMO$^{\Delta hepa}$/JNK$^{\Delta hepa}$ were observed, indicating that hepatocyte differentiation in our model is inhibited in favor of ductular reaction and cholangiocyte differentiation. Of note, JNK1/2-knockout mice have reduced phosphorylation of β-catenin, suggesting that JNK is necessary for β-catenin phosphorylation, as suggested.[31]

Our protein and mRNA data overwhelmingly indicated that overexpression and activation of the EGFR/ErbB2 family was implicated in multistep cystogenesis toward CCA in NEMO$^{\Delta hepa}$/JNK$^{\Delta hepa}$ livers. Indeed, EGFR overexpression occurs in 11%-27% of human CCA, whereas HER2 overexpression is less frequent but very characteristic in transgenic mouse models.[36,48] It has been reported that EGF is released by tumor-associated macrophages (TAM).[49] Binding of EGF to its receptors induces their homodimerization or heterodimerization, which in turn activates downstream signaling pathways that regulate cell differentiation, migration, angiogenesis, and survival.[50] In our study, we specifically focused on RAF-MEK1/2-ERK2 and JAK/STAT signaling. Both pathways were dramatically induced in NEMO$^{\Delta hepa}$/JNK$^{\Delta hepa}$ livers, suggestive of the strong proliferative and inflammatory microenvironment within the hepatic parenchyma.

Therefore, we tested the possibility of blocking EGFR/HER2 signaling as a novel strategy in treating hyperproliferation of the biliary epithelium. We used lapatinib, a dual TKI that efficiently inhibits both EGFR and HER2. Treatment not only prevented RAF-MEK-ERK activation but also inhibited biliary cyst formation. However, its efficacy in clinical translation may highly depend on enrollment of patients with EGFR/HER2 hyperactivation or overexpression.

Recently, Heikenwalder's group showed the therapeutic relevance of inhibiting JNK in CCA both *in vivo* and in cell lines.[12] LPC-specific *Jnk1/2* knockout mice were used in two different CCA models. In contrast to our observations, they found reduced cholangiocellular injury in both models. This apparent discrepancy between both studies may be reconciled considering that adeno-associated virus-mediated *Cre* expression in hepatocytes might not exactly resemble *Alb-Cre* excision since birth, as employed in our study. To further confirm the implications of *Jnk1/2* ablation in hepatocytes, we blocked *Jnk2* specifically in hepatocytes using a liposome-delivery system coupled to an siRNA that was recently reported by our laboratory.[16] Our data undoubtedly indicated that *Jnk1/2* in hepatocytes prevents biliary cell hyperproliferation. In addition, lapatinib successfully prevented activation of the EGFR-RAF-MEK1/2-ERK1/2 pathway in *Jnk1/2* mice. However, more studies (e.g, assessment of JNK levels *in vitro* and in organoids) need to be performed to better define the specific role of JNK for CCA initiation.

Overall, our results show that complete inhibition of JNK signaling in hepatocytes in an experimental HCC model triggers binding of EGF (most likely released by the increased TAM-derived environment) to its receptor activating EGFR-RAF-MEK1/2-ERK1/2 signaling. This cascade is essential to drive EMT transdifferentiation of oval cells into biliary cells and massive ducto/cystogenesis, which shares the molecular features of CCA. Here, CAF-derived cytokines, including *tnf* or transforming growth factor beta (*tgfβ*), might further contribute to exacerbated proliferation of biliary cells (Supporting Fig. S14).

Our study better delineates the pathogenesis of CCA by describing a novel function of JNK in cholangiocyte hyperproliferation. It also defines new therapeutic options to inhibit pathways involved in cholangiocarcinogenesis.

REFERENCES

1) Sirica AE, Nathanson MH, Gores GJ, Larusso NF. Pathobiology of biliary epithelia and cholangiocarcinoma: proceedings of the Henry M. and Lillian Stratton Basic Research Single-Topic Conference. Hepatology 2008;48:2040-2046.
2) Thoolen B, Maronpot RR, Harada T, Nyska A, Rousseaux C, Nolte T, et al. Proliferative and nonproliferative lesions of the rat and mouse hepatobiliary system. Toxicol Pathol 2010;38(Suppl.):5S-81S.
3) Zabron A, Edwards RJ, Khan SA. The challenge of cholangiocarcinoma: dissecting the molecular mechanisms of an insidious cancer. Dis Model Mech 2013;6:281-292.
4) Seki E, Brenner DA, Karin M. A liver full of JNK: signaling in regulation of cell function and disease pathogenesis, and clinical approaches. Gastroenterology 2012;143:307-320.
5) Girnius N, Edwards YJ, Garlick DS, Davis RJ. The cJUN NH2-terminal kinase (JNK) signaling pathway promotes genome stability and prevents tumor initiation. Elife 2018;7:e36389.
6) Hubner A, Mulholland DJ, Standen CL, Karasarides M, Cavanagh-Kyros J, Barrett T, et al. JNK and PTEN cooperatively control the development of invasive adenocarcinoma of the prostate. Proc Natl Acad Sci U S A 2012;109:12046-12051.

7) Liu J, Wang T, Creighton CJ, Wu SP, Ray M, Janardhan KS, et al. JNK(1/2) represses Lkb(1)-deficiency-induced lung squamous cell carcinoma progression. Nat Commun 2019;10:2148.
8) Davies CC, Harvey E, McMahon RF, Finegan KG, Connor F, Davis RJ, et al. Impaired JNK signaling cooperates with KrasG12D expression to accelerate pancreatic ductal adenocarcinoma. Cancer Res 2014;74:3344-3356.
9) Cellurale C, Sabio G, Kennedy NJ, Das M, Barlow M, Sandy P, et al. Requirement of c-Jun NH(2)-terminal kinase for Ras-initiated tumor formation. Mol Cell Biol 2011;31:1565-1576.
10) Das M, Garlick DS, Greiner DL, Davis RJ. The role of JNK in the development of hepatocellular carcinoma. Genes Dev 2011;25:634-645.
11) Han MS, Barrett T, Brehm MA, Davis RJ. Inflammation mediated by JNK in myeloid cells promotes the development of hepatitis and hepatocellular carcinoma. Cell Rep 2016;15:19-26.
12) Yuan D, Huang S, Berger E, Liu L, Gross N, Heinzmann F, et al. Kupffer cell-derived Tnf triggers cholangiocellular tumorigenesis through JNK due to chronic mitochondrial dysfunction and ROS. Cancer Cell 2017;31:771-789.e6.
13) Das M, Jiang F, Sluss HK, Zhang C, Shokat KM, Flavell RA, et al. Suppression of p53-dependent senescence by the JNK signal transduction pathway. Proc Natl Acad Sci U S A 2007;104:15759-15764.
14) Das M, Sabio G, Jiang F, Rincon M, Flavell RA, Davis RJ. Induction of hepatitis by JNK-mediated expression of TNF-alpha. Cell 2009;136:249-260.
15) Cubero FJ, Zoubek ME, Hu W, Peng J, Zhao G, Nevzorova YA, et al. Combined activities of JNK1 and JNK2 in hepatocytes protect against toxic liver injury. Gastroenterology 2016;150:968-981.
16) **Zoubek ME**, **Woitok MM**, Sydor S, Nelson LJ, Bechmann LP, Lucena MI, et al. Protective role of c-Jun N-terminal kinase-2 (JNK2) in ibuprofen-induced acute liver injury. J Pathol 2019;247:110-122.
17) **Cubero FJ**, **Singh A**, Borkham-Kamphorst E, Nevzorova YA, Al Masaoudi M, Haas U, et al. TNFR1 determines progression of chronic liver injury in the IKKgamma/Nemo genetic model. Cell Death Differ 2013;20:1580-1592.
18) Luedde T, Beraza N, Kotsikoris V, van Loo G, Nenci A, De Vos R, et al. Deletion of NEMO/IKKgamma in liver parenchymal cells causes steatohepatitis and hepatocellular carcinoma. Cancer Cell 2007;11:119-132.
19) **Cubero FJ**, **Zhao G**, Nevzorova YA, Hatting M, Al Masaoudi M, Verdier J, et al. Haematopoietic cell-derived Jnk1 is crucial for chronic inflammation and carcinogenesis in an experimental model of liver injury. J Hepatol 2015;62:140-149.
20) Grasl-Kraupp B, Ruttkay-Nedecky B, Koudelka H, Bukowska K, Bursch W, Schulte-Hermann R. In situ detection of fragmented DNA (TUNEL assay) fails to discriminate among apoptosis, necrosis, and autolytic cell death: a cautionary note. Hepatology 1995;21:1465-1468.
21) **Cubero FJ**, **Peng J**, Liao L, Su H, Zhao G, Zoubek ME, et al. Inactivation of caspase 8 in liver parenchymal cells confers protection against murine obstructive cholestasis. J Hepatol 2018;69:1326-1334.
22) Seehawer M, Heinzmann F, D'Artista L, Harbig J, Roux PF, Hoenicke L, et al. Necroptosis microenvironment directs lineage commitment in liver cancer. Nature 2018;562:69-75.
23) Ehedego H, Boekschoten MV, Hu W, Doler C, Haybaeck J, Gabetaler N, et al. p21 ablation in liver enhances DNA damage, cholestasis, and carcinogenesis. Cancer Res 2015;75:1144-1155.
24) Willenbring H, Sharma AD, Vogel A, Lee AY, Rothfuss A, Wang Z, et al. Loss of p21 permits carcinogenesis from chronically damaged liver and kidney epithelial cells despite unchecked apoptosis. Cancer Cell 2008;14:59-67.
25) Affo S, Yu LX, Schwabe RF. The role of cancer-associated fibroblasts and fibrosis in liver cancer. Annu Rev Pathol 2017;12:153-186.
26) Park SY, Roh SJ, Kim YN, Kim SZ, Park HS, Jang KY, et al. Expression of MUC1, MUC2, MUC5AC and MUC6 in cholangiocarcinoma: prognostic impact. Oncol Rep 2009;22:649-657.
27) Mu X, Pradere JP, Affo S, Dapito DH, Friedman R, Lefkovitch JH, et al. Epithelial transforming growth factor-beta signaling does not contribute to liver fibrosis but protects mice from cholangiocarcinoma. Gastroenterology 2016;150:720-733.
28) Isomoto H, Mott JL, Kobayashi S, Werneburg NW, Bronk SF, Haan S, et al. Sustained IL-6/STAT-3 signaling in cholangiocarcinoma cells due to SOCS-3 epigenetic silencing. Gastroenterology 2007;132:384-396.
29) Smigiel JM, Parameswaran N, Jackson MW. Potent EMT and CSC phenotypes are induced by oncostatin-M in pancreatic cancer. Mol Cancer Res 2017;15:478-488.
30) Carpino G, Cardinale V, Folseraas T, Overi D, Floreani A, Franchitto A, et al. Hepatic stem/progenitor cell activation differs between primary sclerosing and primary biliary cholangitis. Am J Pathol 2018;188:627-639.
31) Lee MH, Koria P, Qu J, Andreadis ST. JNK phosphorylates beta-catenin and regulates adherens junctions. FASEB J 2009;23:3874-3883.
32) Andersen JB. Molecular pathogenesis of intrahepatic cholangiocarcinoma. J Hepatobiliary Pancreat Sci 2015;22:101-113.
33) Galdy S, Lamarca A, McNamara MG, Hubner RA, Cella CA, Fazio N, et al. HER2/HER3 pathway in biliary tract malignancies; systematic review and meta-analysis: a potential therapeutic target? Cancer Metastasis Rev 2017;36:141-157.
34) Nam AR, Kim JW, Cha Y, Ha H, Park JE, Bang JH, et al. Therapeutic implication of HER2 in advanced biliary tract cancer. Oncotarget 2016;7:58007-58021.
35) Li L, Zhao GD, Shi Z, Qi LL, Zhou LY, Fu ZX. The Ras/Raf/MEK/ERK signaling pathway and its role in the occurrence and development of HCC. Oncol Lett 2016;12:3045-3050.
36) Chong DQ, Zhu AX. The landscape of targeted therapies for cholangiocarcinoma: current status and emerging targets. Oncotarget 2016;7:46750-46767.
37) Baselga J. Targeting tyrosine kinases in cancer: the second wave. Science 2006;312:1175-1178.
38) Wood ER, Truesdale AT, McDonald OB, Yuan D, Hassell A, Dickerson SH, et al. A unique structure for epidermal growth factor receptor bound to GW572016 (Lapatinib): relationships among protein conformation, inhibitor off-rate, and receptor activity in tumor cells. Cancer Res 2004;64:6652-6659.
39) Scaltriti M, Verma C, Guzman M, Jimenez J, Parra JL, Pedersen K, et al. Lapatinib, a HER2 tyrosine kinase inhibitor, induces stabilization and accumulation of HER2 and potentiates trastuzumab-dependent cell cytotoxicity. Oncogene 2009;28:803-814.
40) Blechacz B, Gores GJ. Cholangiocarcinoma: advances in pathogenesis, diagnosis, and treatment. Hepatology 2008;48:308-321.
41) Guest RV, Boulter L, Dwyer BJ, Forbes SJ. Understanding liver regeneration to bring new insights to the mechanisms driving cholangiocarcinoma. NPJ Regen Med 2017;2:13.
42) Eferl R, Ricci R, Kenner L, Zenz R, David JP, Rath M, et al. Liver tumor development. c-Jun antagonizes the proapoptotic activity of p53. Cell 2003;112:181-192.
43) Hui L, Zatloukal K, Scheuch H, Stepniak E, Wagner EF. Proliferation of human HCC cells and chemically induced mouse liver cancers requires JNK1-dependent p21 downregulation. J Clin Invest 2008;118:3943-3953.
44) Sakurai T, Maeda S, Chang L, Karin M. Loss of hepatic NF-kappa B activity enhances chemical hepatocarcinogenesis through

sustained c-Jun N-terminal kinase 1 activation. Proc Natl Acad Sci U S A 2006;103:10544-10551.
45) Kim Y, Kim MO, Shin JS, Park SH, Kim SB, Kim J, et al. Hedgehog signaling between cancer cells and hepatic stellate cells in promoting cholangiocarcinoma. Ann Surg Oncol 2014;21:2684-2698.
46) Mall AS, Tyler MG, Ho SB, Krige JE, Kahn D, Spearman W, et al. The expression of MUC mucin in cholangiocarcinoma. Pathol Res Pract 2010;206:805-809.
47) Zender S, Nickeleit I, Wuestefeld T, Sorensen I, Dauch D, Bozko P, et al. A critical role for notch signaling in the formation of cholangiocellular carcinomas. Cancer Cell 2013;23:784-795.
48) Kiguchi K, Carbajal S, Chan K, Beltran L, Ruffino L, Shen J, et al. Constitutive expression of ErbB-2 in gallbladder epithelium results in development of adenocarcinoma. Cancer Res 2001;61:6971-6976.
49) Lindsey S, Langhans SA. Epidermal growth factor signaling in transformed cells. Int Rev Cell Mol Biol 2015;314:1-41.
50) Schneider MR, Yarden Y. The EGFR-HER2 module: a stem cell approach to understanding a prime target and driver of solid tumors. Oncogene 2016;35:2949-2960.

Author names in bold designate shared co-first authorship.

Supporting Information

Additional Supporting Information may be found at onlinelibrary.wiley.com/doi/10.1002/hep4.1495/suppinfo.